J MATER SCI **41** (2006) 2509–2516

Perimeter analysis of the Von Koch island, application to the evolution of grain boundaries during heating

M. BIGERELLE
Laboratoire de Métallurgie Physique et Génie des Matériaux, Université des Sciences et Technologies de Lille, CNRS UMR 8517, "Equipe Surfaces et Interfaces" ENSAM CER Lille, 8 Boulevard Louis XIV, 59046 Lille Cedex, France; Laboratoire Roberval, FRE 2833, UTC/CNRS, Centre de Recherches de Royallieu, B P 20529-60205 Compiègne, France

A. IOST*
Laboratoire de Métallurgie Physique et Génie des Matériaux, Université des Sciences et Technologies de Lille, CNRS UMR 8517, "Equipe Surfaces et Interfaces" ENSAM CER Lille, 8 Boulevard Louis XIV, 59046 Lille Cedex, France
E-mail: alain.iost@lille.ensam.fr

Published online: 3 March 2006

This paper introduces an analyse of the fractal dimension by Richardson's method. Two different ways to calculate the fractal dimension are presented with their related calculation errors and applied the Von Koch curves. A Monte-Carlo simulation of the evolution of the grains' boundaries when heating shows that the interfaces lose their fractal characteristics as reported in experimental work. This result is interpreted by dissipation of the energy during the evolution of the grain boundary.

1. Introduction

Quantitative observations about microstructures related to mechanical or physical properties give information on the mechanisms involved, and fundamental knowledge about the distribution particles' sizes is essential to industrial processes. In classical studies the shape of the particles is described by stereological parameters such as the mean size, the shape factor, the surface/volume ratio, the connexity [1, 2] and considerable interest has been expressed in quantitative analysis to minimise the subjectivity of visual assessment. However, classical methods do not take into account the Kostron's observation [3] about the dependence of the size and area fraction of microstructural features upon the magnification used to examine the material. In the same way, in Geoscience, Richardson [4] who studied the cartographic boundaries on map surfaces found that the length of the coastline of Britain (L) is not unique but depends on the length of the divider (ε), also called the yardstick, used for the measurement. A straight line with a negative slope results from plotting the length of the coast versus the length of the divider in log-log co-ordinates. Mandelbrot [5] pointed out the fundamental properties of the non-standard scaling law and answered Richardson's question 'How long is the coastline of Britain' when developing the fractal concept. Fractal analysis admits that the concept of length of irregular objects depends on the size of the measuring yardstick.

The divider method, also called the yardstick or the compass method was extensively applied to treat different boundary surfaces such as rain and clouds [6] cerebral cortex of mammals [7] or quantification of crushed talc concentrate [8]. In our main field of interest, i.e. materials, examples can be found in fracture mechanics [9–11], creep [12, 13], wear [14], corrosion [15, 16], solid-liquid interface morphology [17]. The compass method used to measure profiles or perimeter lengths, is often associated with the Slit Island Method (SIM) introduced by Mandelbrot [9, 18]. SIM proceeds from the relationship between the perimeter (P) of the island versus its area (A) related by $\log P = 0.5\ \Delta \log A$, where Δ is the fractal dimension of the island's profile.

Numerous algorithms are reported in literature to measure the length (or perimeter) of a profile (or island) and to calculate the fractal dimension. The validity of these algorithms is often tested on the Von Koch islands, the fractal dimension of which is perfectly known. In spite

*Author to whom all correspondence should be addressed.
0022-2461
DOI: 10.1007/s10853-006-5090-5

of all this attention, some crucial aspects of the problem seem to have been left unsolved and are still under discussion [14, 20–25]. The aim of this paper is to analyse the numerical artefacts of Richardson's method when applied on the Von Koch island [26]. This fractal curve, often used to test algorithms, is chosen because its fractal dimension is perfectly known and is used in fracture mechanics to model the crack branching process during the propagation of running cracks [19] or as fractal model of ruptured surfaces [27]. We then provide an original method to compute the fractal dimension of image features and apply it to Monte-Carlo simulations of grain boundaries when heating.

2. The Von Koch island

2.1. Historical background

In 1904, the Swedish mathematician Helge Von Koch [3] introduced curves, which present two main characteristics:

- There is no way to fit a unique tangent and as a consequence they cannot be differentiated.
- They are self-similar: each part of one curve has the same shape regardless of its size.

The Von Koch curves belong to the important class of fractal curves obtained by Iteration Function System [28, 29] and do not possess any analytical mathematical expression. Therefore because of discretisation, resolution effects or else related to mathematics and statistics we might have difficulty in applying mathematical laws to estimate the fractal dimension on experimental data. Before calculating the fractal dimension of experimental curves, it seems interesting to analyse the artefacts on the well-known Von Koch curves to gauge the effect of these errors.

2.2. The definition of the Von Koch island

The Von Koch triadic island is defined as in Fig. 1a. The initiator is a triangle ($\alpha = 60^\circ$) with side length L_0. The construction consists in replacing each segment of the initiator by the generator (a segment of edge length one third of the initial length) and to repeat this process indefinitely. The first four generations are shown in Fig. 1b.

The length of the Von Koch island (perimeter P) is first determined by the following procedure:

Initial:	$P_0 = 3L_0$
First generation:	$P_1 = 3 \times 4 \times \varepsilon_1$, with $\varepsilon_1 = L_0/3$
Second generation:	$P_2 = 3 \times 4^2 \times \varepsilon_2$, with $\varepsilon_2 = \varepsilon_1/3$
nth generation:	$P_n = 3 \times 4^n \times \varepsilon_n$, with $\varepsilon_n = \varepsilon_{n-1}/3$
It follows that:	$4^n = P_n/3\varepsilon_n$ and $3^n = P_0/3\varepsilon_n$

By eliminating n from the above equation it is shown that:

$$P_n = P_0^D \, (\varepsilon_n)^{1-D} \tag{1a}$$

where $D = \ln 4/\ln 3$ is the self-similarity dimension.

When α is different from 60°, similar reasoning leads to:

$$D = \ln 4/\ln\left[2\,(1+\cos\alpha)\right] \tag{1b}$$

When calculating the length with a measuring yardstick η, Equation 2 and 3 are often reported in bibliography:

$$P(\eta) = P_0^D \, (\eta)^{1-D} \tag{2}$$

$$P(\eta) = P_0 \, (\eta)^{1-D} \tag{3}$$

The fractal dimension is a constant related to the slope of the linear form of Equations 2 and 3 plotted in log-log co-ordinates.

These formulations may lead to a false interpretation of the physical process. Equation 2 is true only if $\eta \in H$ where $H = \{\frac{L_0}{3}, \frac{L_0}{3^2}, \ldots \frac{L_0}{3^n}\}$. This set is discreet meaning that Equation 2 is almost never true and will always be false if the graph is not defined by a set of segments of equal lengths (like the circle). This relation will be true to the limit (small $\eta \in H$) by applying the Minkowski Bouligand dimension, noted Δ, [18, 28] defined by:

$$\Delta = \lim_{\eta \to 0} \left[\frac{\ln N(\eta)}{\ln |\eta|} \right] \tag{4}$$

where $N(\eta)$ is the number of segments used to recover the curve.

For the Von Koch island, Equation 2 gives $\Delta = \lim_{n\to\infty} [\frac{\ln 4^n}{\ln |L_0/3^n|}] = \ln 4/\ln 3 = D$. The fractal dimension and the self-similarity dimension are exactly the same only if the yardstick's length is the generator corresponding to the nth iteration, if n tends to infinity and if there is no recovering during the creation of the fractal. As some recovering can appear during the fractal construction, which artificially increases the computational length,

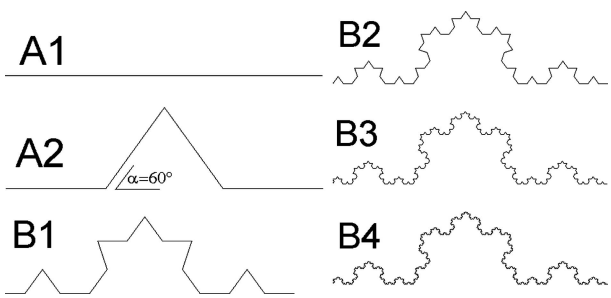

Figure 1 The triadic Von Koch island. (a) the initiator (A1), the generator and its application (A2) and (b) first (B1), second (B2), third (B3) and fourth (B4) iterations.

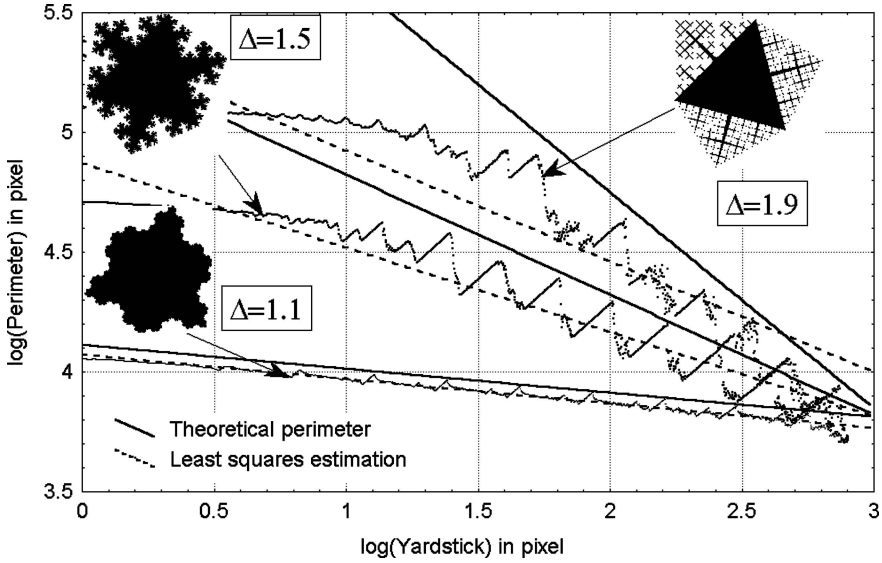

Figure 2 Variation of the perimeter length versus the yardstick size (in log-log co-ordinates) for a triadic 3 Von Koch island with a Self-similarity dimension $D = 1.1$, 1.5 and 1.9. The island is defined on a 2048 × 2048 pixel grid shown on the graph. The continued line represents the theoretical perimeter and the doted one the regression line.

the self-similarity dimension may be higher than the fractal dimension. Tricot [28] has proposed a criterion that does not apply to the stochastic fractal curves encountered in the Material Science. The calculation of the fractal dimension will be very hard to process [30] when recovering appears. Equation 3 (where P_o is a constant) proposed by Richardson [4] and quoted by Mandelbrot [31] does not respect the dimension equation. Indeed the dimension of the left part of Equation 3 is length and that of the right part is $(\text{length})^{1-D}$. This form is inaccurate for algebric calculations in analytical relations where scaling factors are introduced.

3. Numerical analyses

In this study, all curves investigated are defined by a 2048 × 2048 resolution pixels which corresponds to the current resolution of a CCD camera used to record the material morphology by optical microscopy. The Iterated Function System [28] is used to create fractal curves. We first define the co-ordinates of the initiator (polygon) and of the generator. Secondly the number of iterations (or steps) used to construct the Von Koch curves (or another fractal curves) is manually chosen, and finally the Von Koch curves are created by a recursive procedure using vectorial notation. At the end of the last iteration, the fractal is defined by a set of co-ordinates. Thanks to this vectorial representation, the curve is constructed without any discretisation error (neglecting the error in the representation number). The number of co-ordinates of the Von Koch flake obtained by iterations for a p-sided polygon initiator is given by $p \times 4^i$. Then a resolution of image is chosen ($n \times n$ pixels) and the fractal image is built by connecting each successive co-ordinate by a segment. At this stage, discretisation error appears. At least, images are generated and saved in PCX version 5 graphic format. This format is recognised by a high number of graphic viewers, image conversion, or image analysis programs and then allows us different treatments (note that usual software is generally limited in resolution size. . .). We shall now produce some triadic Von Koch flakes with fractal dimensions varying from 1.1 to 1.9, and discretised in 2048×2048 pixels with a yardstick size varying from 1 to 800 pixels. Fig. 2 represents the variation of the perimeter length versus the yardstick size for fractal dimensions 1.1, 1.5 and 1.9. For short yardsticks, the perimeter is more and more underestimated as the fractal dimension increases. The length of the underestimation range increases exponentially with the fractal dimension. This can be explained by the fact that the fractal dimension increases with the length of the initiator and consequently with the size of the lowest number of ε_n in the Koch construction. Let ε_n be the size of the final yardstick after n iterations of the Koch construction. With the same mathematical statements as in Equation 1, $D = \ln 4/\ln[2(1+\cos\alpha)]$ and $\varepsilon_n = L_0/[2(1+\cos\alpha)]^n$ and eventually:

$$\varepsilon_n = L_0/10^{\frac{n\log 4}{\Delta}} \tag{5}$$

Then a second software is used to calculate the perimeter length $P(\eta)$ with a measuring yardstick η.

Two methods can be stated to estimate the slope of the log-log plot:

TABLE I Values of the fractal dimension obtained from Von Koch islands of different theoretical fractal dimensions Δ_t shown in Fig. 2. The calculated fractal dimensions Δ_c are evaluated from the two numerical methods described in the text $\eta_{\min}$ and $\eta_{\max}$ represent the domains of the yardstick variation (in pixels) when fractal dimension is estimated

Method	ARYV			MSMV		
(Δ_t)	Δ_c	$\eta_{\min}$	$\eta_{\max}$	Δ_c	$\eta_{\min}$	$\eta_{\max}$
1.1	1.102	1	800	1.099	1	580
1.2	1.181	1	800	1.183	2	573
1.26	1.224	1	800	1.231	2	609
1.3	1.248	1	800	1.267	4	619
1.4	1.306	1	800	1.352	5	645
1.5	1.352	1	800	1.438	7	672
1.6	1.389	1	800	1.537	14	691
1.7	1.417	1	800	1.644	24	717
1.8	1.439	1	800	1.737	30	737
1.9	1.462	1	800	1.826	35	755

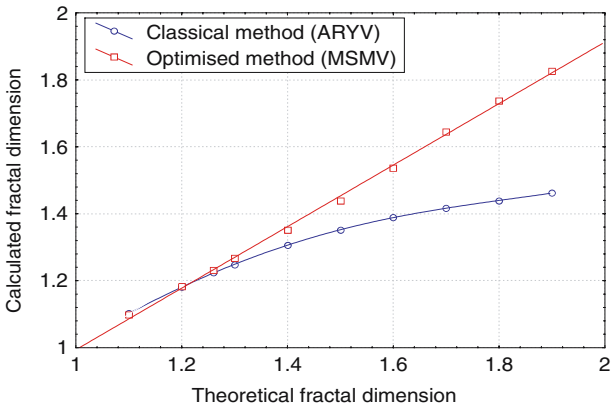

Figure 3 Values of the fractal dimension obtained from Von Koch islands of different theoretical fractal dimensions Δ_t shown in Fig. 2. The calculated fractal dimensions Δ_c are evaluated from the two numerical methods described in the text.

3.1. Method one: all range of the yardstick variation (ARYV)

The slope is calculated taking all the perimeters computed with different ruler lengths varying from 1 to 800 pixels. Table I shows that the fractal dimension is more and more underestimated as the fractal dimension increases. That can be explained by the fact that ε_5 increases with the fractal dimension and that the part of underestimation of the perimeter decreases the slope of the log-log plot. The calculated fractal dimensions are lower than 1.5. This method is not accurate to calculate the highest fractal dimensions and the yardstick range cannot be chosen at random to estimate the fractal dimension as accurately as possible (Fig. 3).

3.2. Method two: the maximal slope with minimal variation (MSMV)

To evaluate the set of perimeters that is significantly less than the expected one, the following method is used:

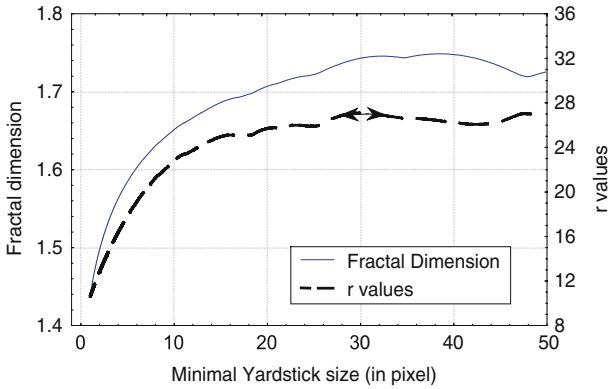

Figure 4 Values r_j and Δ_i versus the minimal size of η_i (in pixel) for the Von Koch of theoretical fractal dimension of 1.8. We obtain $r_{\max} = 27.5$ those give a fractal dimension of $\Delta_{\max} = 1.74$.

Let $E = \{(\log \eta_1, \log P(\eta_1)), (\log \eta_2, \log P(\eta_2)), \ldots, (\log \eta_n, \log P(\eta_n))\}$ with $\eta_1 < \eta_2 < \eta_n$ be the set of the log-log plot. The Fractal dimension Δ_j is calculated by the linear least square method from the set $E_j = \{(\log \eta_j, \log P(\eta_j)), (\log \eta_{j+1}, \log P(\eta_{j+1})), \ldots, (\log \eta_n, \log P(\eta_n))\}$. As the perimeter is underestimated for small yardsticks, the fractal dimension increases with increasing j until a critical value corresponding to the first significant oscillation in the log-log plot. To avoid absurd points that will increase the slope artificially, the standard deviation of the fractal dimension is minimised, the unbiased standard deviation s_j of the residuals (observed perimeter minus calculated perimeter with the slope $1 - \Delta_j$) is computed and the following estimator $r_j = \frac{\Delta_j}{s_j}$ (which seems a ratio signal—noise) is built. By calculating all r_j from all the sets E_j (with $1 \leq j < n$, n is given by ε_1 according to Equation 5), $\Delta_{\max}$ is obtained for the first highest value $r_{\max}$. Fig. 4 represents r_j and Δ_j versus the minimal yardstick size for the Von Koch flake with a 1.8 theoretical fractal dimension. As we found $r_{\max} = 27.5$ (which gives a fractal dimension of $\Delta_{\max} = 1.74$) the yardstick must be higher than 30 pixels to estimate precisely the fractal dimension. Table I shows that ε_5 (column $\eta_{\min}$, method 3) matches well with the shortest segment of the

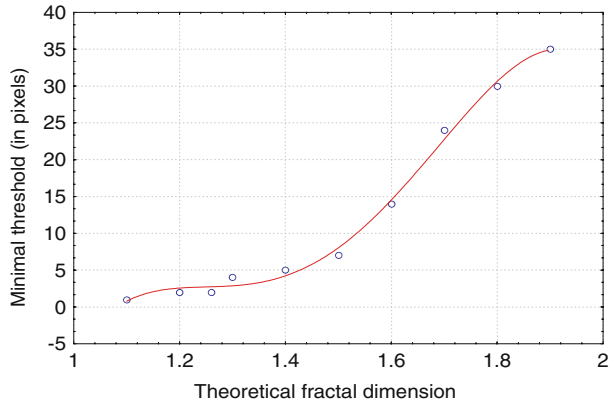

Figure 5 Evolution of $\eta_{\min}$ versus the theoretical fractal dimension.

Von Koch flakes ε_5 obtained by the flake constructor. It is then possible by this algorithmic method to approach the values of ε_5 without knowing the fractal construction parameter (Fig. 5). However, ε_1 is imposed by the fractal construction parameter and this method could not be applied without knowing ε_1 i.e. the largest segment of the fractal constructor.

4. Monte Carlo simulation of diffusion on the Von Koch flakes

We propose to analyse the evolution of the grains' boundaries when heating by using a fractal model of diffusion on a fractal interface. Many analytical models allow us to represent the evolution of the grain size when heating. These models, which suppose that profiles can be derived to integrate differential equations, do not apply to fractal surfaces. In most of these models, the equations contain the radius of the grain. However, a local radius has no physical or mathematical sense for a fractal interface. As a consequence, analytical models do not include the fractal aspect of the interface. No differential equation can be stated for these particular interfaces and we have decided to model the evolution of the interface when heating by a Monte Carlo simulation.

Experimental work related to the evolution of the fractal dimension of the grains' boundaries when heating are reported in literature. Rubio *et al.* [35] have studied the effect of heating on the fractal dimension of a ZrO_2 powder. When heating from 125°C up to 1000°C at the rate of 1°C/mn the fractal dimension is experimentally found to decrease from 1.84 to 1.47. Tanaka [36, 37] shows that the fractal dimension of grain interface is correlated with the fractal dimension of the ruptured surface for six different materials. Streitenberger *et al.* [38] have measured the fractal dimension of Zn grains when heating for 15′ at 696° C, 796°C or 896°C. For this last temperature, they noted that Δ decreases from 1.15 to 1.04 and concluded that the initial fractal dimension of the interface plays an important part in the kinetics of the diffusion process.

4.1. The Monte Carlo model

The algorithm used to simulate diffusion at the grain boundary was first developed by Anderson *et al.* [39]. The grain structure is modelled by a matrix, each element of which, we called cell, is affected by a spin that represents the grain orientation. The Monte Carlo simulation can be summed up by 6 steps:

1. A cell (i, j) of the matrix of size n^2 is chosen at random.
2. The energy of the spin is calculated according to the Hamiltonien $E_{i,j} = -J \sum_{k=1}^{6} \delta_{Si,j,Sk}$.

where $E_{i,j}$ is the energy of the cell (i, j), J the interfacial energy of the grain, S_k the cells neighbouring (i, j) and $\delta_{Si,j,Sk}$ the kronecker symbol (=1 if spin k equals the spin of the (i, j) cells and zero elsewhere).

3. A new spin is chosen at random.
4. If the energy of the spin is minimised then the spin of the cell (i,j) is changed,
5. Steps 1 to 4 are repeated n^2 times and represent 1 MCS (Monte Carlo Step).
6. Then another MCS is constructed by repeating steps 1 to 5 and so on.

4.2. The software

A computer program was developed in order to simulate the Monte Carlo algorithm in the C++ language. At different MCS, an image in PCX format is put out and our algorithm described earlier is used to calculate the different fractal parameters. The software is optimised to store only in memory the co-ordinates of the interface thanks to a double list of pointers.

4.3. Modelling of the initial fractal grain structure

During solidification, the grain interface presents a fractal structure [40, 41]. To construct such fractal boundaries, Von Koch island, with $D = 1.5$, are duplicated to obtain an image size of 3000 × 2000 pixels with five iterations of the generator (Fig. 6). The central flake is centred on the matrix and the borders of the matrix join the adjacent grains. We can admit that during the heating phase, the interface energy is minimised, and with such a configuration, the central grain area is constant when simulating the heating process.

4.4. Monte Carlo simulation

The 8192 steps of the Monte Carlo simulation take around 10 min on a Pentium 2 GHz with 512 Mo memory. Fig. 6 represents the evolution of the fractal grain when heating for different MCS (64, 128, 512, 2048, 8192 MCS). The following remarks can be stated from this simulation:

1. The grain area is constant during the simulation. Adjacent grains are pinned and no grain growth occurs.
2. No anisotropy arises during the simulation.
3. As time increases, the fractal curve looks like a Von Koch flake with fewer and fewer iterations. Diffusion successively erodes the shape created by the iterations of the initial Von Koch flake and all the generation steps of the Von Koch island are found as heating time increases.

4.5. Calculation of the fractal dimension

The perimeter is then computed for different heating times and yardstick lengths. Fig. 7 represents the variation of the

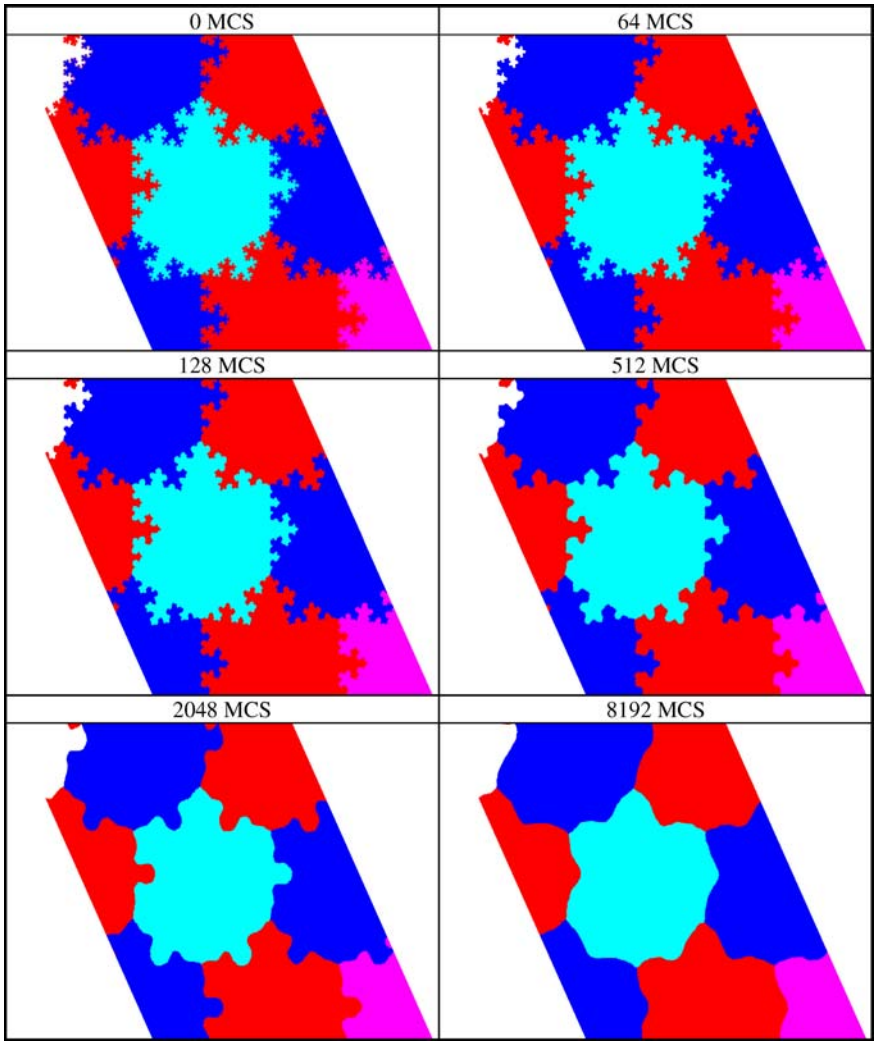

Figure 6 Heating simulation by Monte Carlo method. The initial fractal dimension of the shape is 1.5 with five iterations of the generator. Figures show effect of heating for 64, 128, 512, 2048 and 8192 Monte Carlo Steps (MCS).

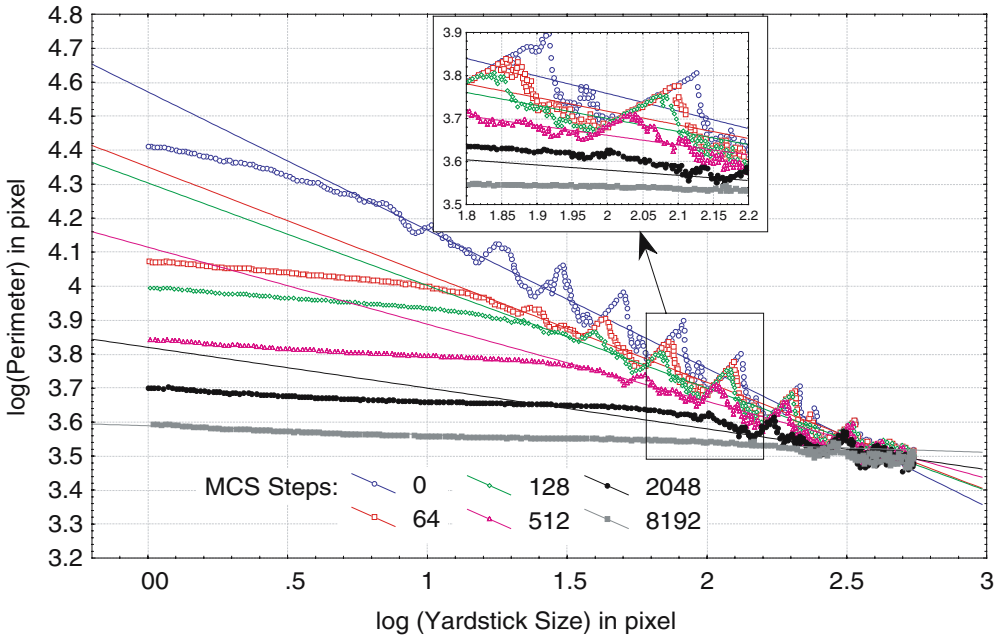

Figure 7 Variation of the perimeter length versus the yardstick size (in log-log co-ordinates) for a Von Koch island with a Self-similarity dimension $D = 1.5$. The continued line represents the regression line using the MSMV method for fractals described in Fig. 6.

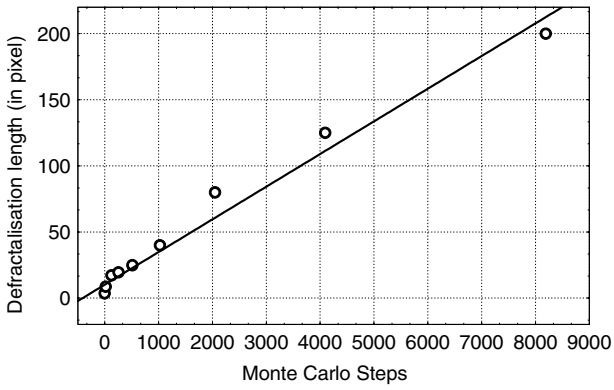

Figure 8 The threshold of defractalisation in pixel versus the MCS heating time.

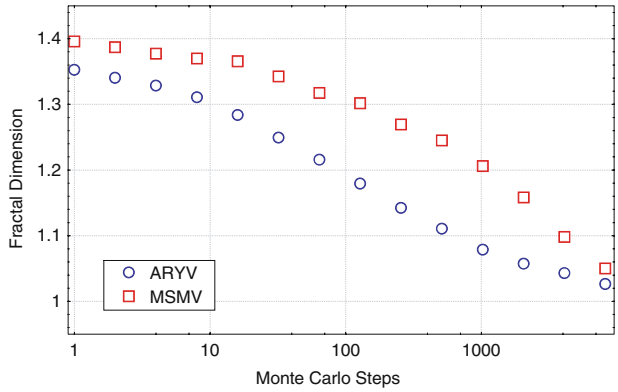

Figure 9 Values of the fractal dimension calculated by both the ARYV and MSMV method versus the MCS heating time.

perimeter versus the yardstick length for different heating times in MCS. Five important remarks have to be stated:

1. For a given yardstick length, the measured perimeter decreases with the heating time since the diffusion process decreases the apparent surface energy. As a consequence, the perimeter is minimised as the heating time increases whatever the scale of the measure.
2. For infinite heating times (here 8192 MCS) the grains tend to a hexagonal form that represents the equilibrium state. Energy is used by mass transport to smooth the interface without increasing the grain size, and every model of grain growth must include this mass transport. This result can explain why all models that do not include the mesoscopic geometry of interfaces overestimate the experimental growth law [33].
3. When the heating time increases, the perimeter becomes constant for a large range of small yardsticks, meaning that $\Delta = 1$ and that the interface is seen as Euclidean in this scale range. The threshold between the fractal regime and the Euclidean one is determined and Fig. 8 represents the variation versus heating time. A linear relation is found: $\varepsilon_c = 0.025_{\pm 0.002} t_{MCS} + 10_{\pm 5}$ with a correlation coefficient of $r = 0.99$.

As MCS step is proved proportional to the real heating time [42–45], we can infer that the scale length range in which we can admit the interface as non-fractal varies linearly with the heating time. Then, it becomes obvious that the definition of self-affinity does not hold and that Equation 1 to 3 can not be used to calculate the fractal dimension. Consequently, Richardson's method cannot be applied to calculate the fractal dimension of grains' boundaries, while Equation 4 can. However, Equation 4 can only be used analytically and no numerical estimation can be found.

Nevertheless a local fractal dimension can be calculated by Richardson's method by plotting the regression line including points after the threshold. This line is drawn in Fig. 7. It is then possible to plot the fractal dimension calculated without taking or not into consideration the threshold (Fig. 9). The least important fractal dimension without threshold (ARYV) results from the loss of fractality of the perimeter for the short yardstick length. After this threshold, the linear relation can approximate the relation between the perimeter and the yardstick size (in log-log co-ordinates). In both cases, Δ decreases when the heating time rises. Even after the threshold, the fractal dimension decreases because some parts of the fractal have been eroded by diffusion, which minimises the perimeter's length. The fractal dimension converges to 1 meaning that the fractal tends to become Euclidean curve.

By analysing the different extrema in the log-log plot, it is shown that the peaks' amplitude decreases with heating time (Zoom in Fig. 7). For a given heating time, the decrease is more and more important as the yardstick size decreases. As we have proved that the maxima allow us to approximate the real perimeter, this result proves that the fractal dimension depends on the scale of measurement. However, curves are also fractal but do not possess the self-similarity structure of the initial Von Koch island. Then the local fractal dimension has to be computed. For these calculations, the method described above does not hold because the curve is not self-similar. Therefore, the local fractal dimension is calculated by the regression between two adjacent peaks. The values of this local fractal dimension are shown in Fig. 10 for different po-

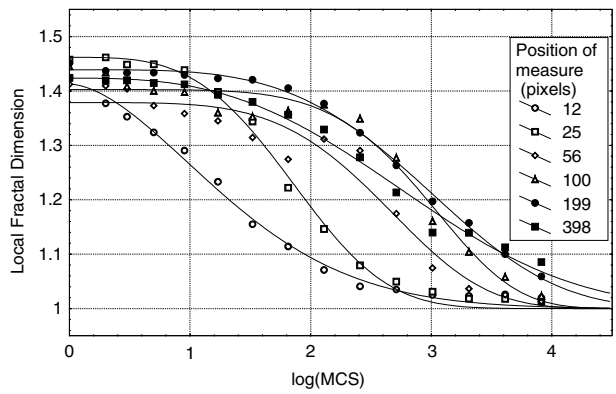

Figure 10 Calculation of the local fractal dimension through the regression line between two adjacent peaks shown in Fig. 7 for different MCS heating times.

sition of the peak. We remark that for a given positions of the peak the local fractal dimension decreases with the heating time to tend to the Euclidean dimension ($D = 1$). For a given heating time, the fractal dimension decreases with decreasing the length of the yardstick. This fact confirms that the fractal curve loses its fractality at small scale and keeps the fractality at a higher scale.

5. Conclusion

In this paper, we carried out a numerical analysis of Richardson's method. It was shown that this method is adequate to calculate the fractal dimension of self-similar structure but inappropriate to calculate the fractal dimension of smooth forms. Some artefacts may appear if self-similarity is not respected. It was shown that a correlation might appear between the fractal dimension and some shape factors of the images. Therefore, if some shape parameters are correlated with a physical process (grain size for example) then the correlation between a physical process and the fractal dimension may be found as a consequence of the non-respect of self-similarity. Thanks to an original method, the analysis of the perimeter versus the yardstick size allows us to extract the parameter for the construction of the fractal curve. Our algorithm becomes an inverse method that can be applied to detect critical experimental features.

Using Monte Carlo simulations, we have shown that the fractal dimension of a grain interface loses its fractality and its self-similar structure related to the dendritic solidification during the heating process. The fractal dimension varies with the measurement scale. It is often reported by analytical models, which do not include the fractal structure of the interface, that the grain growth follows the power law $\emptyset = a\, t^{0.5}$. However, the power exponent over estimates the experimental law. Energy is consumed to destroy the fractality without any motion of the interface. Some simulations are involved to quantify the effect of the fractal aspect on the motion of the interface and to build other power laws. These results would be mentioned in to another paper.

Acknowledgements

We wish to thank Véronique Hague for her assistance in English

References

1. M. COSTER and J. L. CHERMANT, "Precis d'analyse d'images", (Edition du CNRS, Paris, 1985).
2. M. COSTER and J. L. CHERMANT, *International Metals Reviews* (1983) 228.
3. H. KOSTRON, *Arch Metallkd.* **3**(6) (1949) 193.
4. L. F. RICHARDSON, *General Systems Yearsbook* **6** (1961) 139.
5. B. B. MANDELBROT, *Science* **155** (1967) 636.
6. S. LOVEJOY, *Science* **216** (1982) 185.
7. H. ELIAS et D. SCHARTZ, *Ibid.* **166** (1969) 111.
8. L. O. FILIPPOV and R. JOUSSEMET, *Powder Technology* **105** (1999) 106.
9. B. B. MANDELBROT, D. E. PASSOJA and A. J. PAULLAY, *Nature* **308** (1984) 721.
10. ANNAMARIA CELLI, ANTONELLA TUCCI and LEONARDO ESPOSITO, *Journal of European Ceramic Society* **19**, 441.
11. C. S. PANDE, L. E. RICHARDS, N. LOUAT, B. D. DEMPSEY and A. J. SCHWOEBLE, *Acta Met.* **35** (7) (1987) 1633.
12. X. WANG, H. ZHOU, Z. H. WANG, M. S. TIAN, Y. S. LIU and Q. P. KONG, *Materials Science and Engineering A* **A266** (1999) 250.
13. M. TANAKA, A. KAYAMA, Y. ITO and R. KATO, *J. Mater. Sci.* **33** (1998) 3351.
14. G. W. STACHOWIAK, *Tribology International.* **31**(1–3) (1998) 139.
15. C. M. SUROWIC and T. B. JONES, *Part. Part. Syst. Charact.* 257.
16. F. JIN and F. P. CHIANG, *Res. Nondestr. Eval.* (1996) 229.
17. L. SUN, L. DONG, J. ZHANG and Z. HU, *J. Mater. Sci. Lett.* **16** (1997) 505.
18. B. B. MANDELBROT, "The fractal Geometry of Nature" (Freeman, 1983).
19. L. WEISHENG and C. BINGSEN, *International Journal of Fracture* (1994) R65.
20. H. XIE, *Ibid.* (1989) 267.
21. L. WEISHENG and C. BINGSEN, *International Journal of Fracture* (1994) R29.
22. M. ISSA, M. HAMMADA and A. CHUDNOVSKY, *Ibid.* (1993) 97.
23. M. ISSA, M. HAMMADA and A. CHUDNOVSKY, *Ibid.* (1994) R37.
24. A. IMRE, *Scripta Metallurgica et Materialia* **27** (1992) 1713.
25. *Idem. Physical review B* (1995) 16470.
26. H. VON KOCH, *Arkiv För Matematik* **1** (1904) 681.
27. Z. P. BAZANT, *Journal of Engineering Materials and Technology* (1995) 361.
28. C. TRICOT, "Courbes et dimension fractale" (Springer, Paris, 1993).
29. H. O. PEITGEN, H. JÜRGENS, and D. SAUPE, "Chaos and Fractals New Frontiers of Science" (Springer-Verlag).
30. G. CHERBIT, "Fractal dimensios non entière et applications" (MASSON, Paris, 1991.)
31. B. MANDELBROT, "Les objets fractals" (Flammarion, Paris, 1989).
32. T. B. KIRK, G. W. STACHOWIAK, *et al.*, *Wear* (1991) 347.
33. M. BIGERELLE, Thesis, Caractérisation des Surfaces et Interfaces, Application des fractales en Métallurgie, Lille (1998).
34. N. K. MYSHKIN, A. Y. GRIGORIEV, *et al. Wear* (1992) 119.
35. F. RUBIO, J. RUBIO, J. L.OTEO Effect of heating on the surface fractal dimension of ZrO_2, *Journal of Materials Science Letters* (1997) 49.
36. M. TANAKA, *Journal of Materials Science* (1993) 5753.
37. *Idem. Zeitschrifft Für Metallkunde* (1993) 697.
38. P. STREITENBERGER, D. FÖRSTER, G. KOLBE and P. VEIT, *Scripta Materialia* (1996) 111.
39. M. P. ANDERSON, D. J. SROLOVITZ, G. S. GREST, P. S. SAHNI, *Act. Metall.* **32**(5) (1984) 783.
40. H. E. STANLEY, dans *Fractals and Desordered System* (Springer, 1996) Vol. 1.
41. J. NITTMANN and H. E. STANLEY, *Nature* **321** (1986) 663.
42. S. LING and M. P. ANDERSON, *Mat. Sci. Forum.* **39** (1992) 94.
43. B. RADHAKKRISHAN and T. ZACHARIA, "Modeling and Control of Joining Processes" (AWS, Miami, Florida, 1993).
44. Y. SHEN, "Masterís thesis" (University of Alabama, Birmingham, 1993).
45. J. GAO, and R. G. THOMSON, *Acta Mater.* **44** (1996) 4565.

Received 22 May 2003
and accepted 22 June 2005